Structural and functional changes following brain surgery in pediatric patients with intracranial space-occupying lesions

Xueyi Guan
Beijing Tiantan Hospital
Wenjian Zheng
Beijing Tiantan Hospital
Kaiyu Fan
Beijing Tiantan Hospital
Xu Han
Beijing Tiantan Hospital
Bohan Hu
Beijing Tiantan Hospital
Xiang Li
Beijing Tiantan Hospital
Zihan Yan
Beijing Tiantan Hospital
Zheng Lu
Beijing Tiantan Hospital
Jian Gong
gongjian88@tom.com

Beijing Tiantan Hospital https://orcid.org/0000-0003-3224-9997

Research Article

Keywords: brain tumors, intracranial space-occupying lesions, frontal lobe, brain imaging, cognitive assessment

Posted Date: July 5th, 2022

DOI: https://doi.org/10.21203/rs.3.rs-1748500/v1

Version of Record: A version of this preprint was published at Brain Imaging and Behavior on February 20th, 2024. See the published version at https://doi.org/10.1007/s11682-023-00799-x.

Abstract

We explored the structural and functional changes of the healthy hemisphere of the brain after surgery in children with intracranial space-occupying lesions. We enrolled 32 patients with unilateral intracranial space-occupying lesions for brain imaging and cognitive assessment. Voxel-based morphometry and surface-based morphometry analyses were used to investigate the structural images of the healthy hemisphere. Functional images were analyzed using regional homogeneity, amplitude of low-frequency fluctuations, and fractional-amplitude of low-frequency fluctuations. Voxel-based morphometry and surface-based morphometry analysis used the statistical model built into the CAT12 toolbox. Paired t-tests were used for functional image and cognitive test scores. For structural image analysis, we used family-wise error correction of peak level ($p < 0.05$), and for functional image analysis, we use Gaussian random-field theory correction (voxel $p < 0.001$, cluster $p < 0.05$). We found an increase in gray matter volume in the healthy hemisphere within six months postoperatively, mainly in the frontal lobe. Regional homogeneity and fractional-amplitude of low-frequency fluctuations also showed greater functional activity in the frontal lobe. The results of cognitive tests showed that psychomotor speed and motor speed decreased significantly after surgery, and reasoning increased significantly after surgery. We concluded that in children with intracranial space-occupying lesions, the healthy hemisphere exhibits compensatory structural and functional effects within six months after surgery. This effect occurs mainly in the frontal lobe and is responsible for some higher cognitive compensation. This may provide some guidance for the rehabilitation of children after brain surgery.

Introduction

Brain tumors are the most common solid cancer in children, second only to leukemia as a cause of childhood malignancy; however, the prognosis of many childhood brain tumors has improved recently (Ostrom et al., 2021). Children and adolescents tend to have better survival outcomes than adults for most histologies (Ostrom et al., 2021).For intracranial space-occupying lesions (ISOLs) such as brain tumors, surgery is the main treatment, with subsequent adjuvant therapy after the operation (Louis et al., 2016; Louis et al., 2021).

Brain imaging is important to diagnose diseases and conduct scientific research. Imaging technology has improved recently, and many imaging types have been introduced. T1-weighted imaging is used to explicitly display anatomical details, and voxel-based morphometry (VBM) and surface-based morphometry (SBM) analyses use T1-weighted images to explore structural changes. Resting-state functional magnetic resonance imaging (rs-fMRI) focuses on spontaneous low-frequency fluctuations in the blood oxygen level-dependent (BOLD) signal that is discarded as noise in task fMRI (Lee et al., 2013; Smitha et al., 2017). Many analysis techniques of rs-fMRI provide information regarding the intrinsic activities of the brain (Lv et al., 2018).

Recently, brain imaging technology has been used to study the brain structure and function of healthy people and patients with neurological disease, traumatic brain injury (TBI), epilepsy and mental disease

(Lee et al., 2013; Whitwell, 2009). Similarly, studies have investigated changes in brain function and structure in patients after brain tumor treatment. Xu et al. (Xu et al., 2017) investigated whether contralateral cortical and subcortical structures can actively reorganize themselves in adult brain tumor patients. A study by Almairac et al. (Almairac et al., 2018) in adult insular glioma patients supports the homotopic reorganization theory of plasticity. Liu et al. (Liu et al., 2020) found that the superior parietal lobe in the healthy hemisphere is a key area of cognitive control network in adult tumor patients.

Most studies of pediatric patients after tumor treatment have focused on posterior fossa lesions, and most of the patients involved underwent surgery, radiotherapy, and chemotherapy. Horska et al. (Horská et al., 2010) assessed changes in cerebellar vermis volume in patients with medulloblastoma before and after treatment, and Leung et al. (Leung et al., 2004) conducted a study on children with brain tumors who underwent surgery, radiotherapy, and chemotherapy, and found that the integrity of white matter in the whole brain decreased. Jayakar et al. (Jayakar et al., 2015) conducted a study on children treated for brain tumors and found a decrease in the volume of gray matter, such as in the hippocampus, which may be associated with a decrease in cognitive function.

Previous studies have focused on adult patients with brain tumors, children with posterior fossa tumors, and children with brain tumors undergoing surgery and adjuvant therapy. However, few studies have focused on structural and functional changes in the healthy hemisphere in children and adolescents who undergo surgery alone. We aimed to explore the structural and functional changes of the healthy hemisphere in children and adolescents within six months after surgery for unilateral ISOLs only.

Methods

Participants

Thirty-two unilateral ISOL patients who were admitted to the Department of Pediatric Neurosurgery of Beijing Tiantan Hospital from July 2020 to November 2021 were selected. Preoperative structural and functional scans were performed, as well as cognitive assessments to understand the results of imaging analyses. This was repeated within six months after surgery. We included patients aged 5–18 years with unilateral ISOLs without contralateral invasion, and when brain surgery was required. We excluded patients with the following characteristics: those without informed consent; suffering from hydrocephalus (Evans' index > 0.3); unable to complete brain imaging scans for any reason; with low imaging data quality, such as after excessive head movement, any artifacts, or awful normalization; had a history of TBI, neurosurgery, mental and psychological diseases, genetic metabolic diseases, endocrine system diseases; with contraindications to general anesthesia; and those where we were unable to follow-up.

For structural analysis, all the raw structural data of all 32 patients were visually inspected for potential artifacts before preprocessing (Ying et al., 2020), and one patient was excluded for head motion artifacts. For functional analysis, four patients were excluded due to excessive head movements during scanning.

For cognitive assessment, data could not be obtained for nine children as they did not want to be assessed.

Imaging Data Acquisition

The patients were instructed to remain seated with their eyes closed. No sedation was applied during the examination. All patients underwent MRI scans on a 3T scanner (MAGNETOM Prisma, Siemens Healthcare, Erlangen, Germany) with a 64-channel head/neck coil. The protocol included T1 weighted structure imaging with magnetization prepared rapid acquisition gradient echo (MPRAGE) sequence and rs-fMRI with an echo-planar imaging (EPI) sequence. The scan parameters for the MPRAGE sequence were: TR = 1560 ms; TE = 1.65 ms; flip angle = 8°; slices = 176; field of view (FOV) = 256×256 mm; and voxel size = 1 mm isotropic. The parameters for EPI with simultaneous multislice (SMS) acceleration technique were: TR = 2000 ms; TE = 35 msec; slices = 69; SMS = 3; FOV = 207×207 mm; voxel size = 2.2 mm isotropic; volumes = 240.

Data Preprocessing And Analysis

Structural Data

VBM and SBM processing and analysis were performed using CAT12 (vCAT 12.7) (http://www.neuro.uni-jena.de/cat/) and Statistical Parametric Mapping 12 (SPM 12; v7771 https://www.fil.ion.ucl.ac.uk/spm, developed by members and collaborators of the Wellcome Centre for Human Neuroimaging, Institute of Neurology, University College London) implemented in MATLAB R2020b (MathWorks, Inc.). Before processing, the images with lesions on the right were flipped left and right, so that all the enrolled 31 pairs of images had lesions on the same side, and the subsequent analysis was easier to perform. According to CAT12, we chose the longitudinal model optimized to detect small changes. The toolbox included bias-field and noise removal; skull stripping; and gray matter (GM), white matter (WM), and cerebrospinal fluid (CSF) segmentation. Unified segmentation (Ashburner & Friston, 2005) was selected to perform tissue segmentation. Given that our patients were children and adolescents, we chose a tissue probability map developed for children (Zhao et al., 2019). Afterward, all GM images were normalized to the standard Montreal Neurological Institute (MNI) template using diffeomorphic anatomical registration thorough exponential Lie algebra (DARTEL) to a 1.5 mm isotropic template provided by the CAT12 toolbox (Ashburner, 2007). Finally, normalized GM images were smoothened using an 8 mm full width at half maximum (FWHM) Gaussian kernel, and a variety of surface indices provided by the toolbox were calculated, including thickness, depth, gyrification, and fractal dimension (FD).

Functional Data

Data processing and analysis of brain imaging (DPABI; v6.0, http://rfmri.org/dpabi) and SPM 12 (https://www.fil.ion.ucl.ac.uk/spm), implemented in MATLAB R2020b (MathWorks, Inc.), were used to

preprocess fMRI images (Chao-Gan & Yu-Feng, 2010; Yan et al., 2016). The first 10 images were discarded, and slice-timing correction and head motion correction were implemented. The data of subjects whose head movement translation was > 3 mm or rotation was > 3° were discarded. Further, the functional image was redirected to the standard MNI space by DARTEL (Ashburner, 2007) and the 3 mm cube was resampled. The linear trend, CSF signal, WM, and Friston 24-parameter head motion model were regressed as cumulative covariates from the BOLD signal (Friston et al., 1996) (covariate regression of global signals was not used during preprocessing (He & Liu, 2012; Saad et al., 2012)). Next, the images were smoothed with FWHM 4×4×4 and band-pass filtering (0.01–0.10 Hz) performed. During the preprocessing, three indices of functional separation were calculated by the toolbox as follows: Regional homogeneity (Reho) (before smoothing); amplitude of low frequency fluctuation (ALFF); and fractional-ALFF (fALFF) (before filtering). These underwent Fisher Z-transformation prior to statistical analysis.

Cognitive Assessment

CNS Vital Signs (CNS VS) is a complex computerized neurocognitive test battery with various cognitive domains developed as a routine clinical screening instrument (Gualtieri & Johnson, 2006). The battery can provide a subject with a 30–40 minute evaluation and generate a report with age-adjusted standard scores for 15 domains that are derived from 10 subtests, including composite memory, verbal memory, visual memory, psychomotor speed (PsyMoSp), and reaction time, complex attention, cognitive flexibility, processing speed, and executive function, social acuity, reasoning, working memory, and sustained attention, simple attention, and motor speed (MS). Based on these scores, a neurocognition index (NCI), which is a general assessment of the overall neurocognitive status of the patient, was generated. The CNS VS standard scores have a mean of 100 and a standard deviation of 15. Patient cognitive assessments were performed with the CNS VS battery preoperatively, and a brain scan was performed within 1 week. This was repeated within 6 months after surgery.

Statistical Analysis

According to CAT12, we selected the Flexible Factorial design in the SPM statistics module and set parameters accordingly. In the “Explicit Mask,” we choose a self-made GM binary mask of the right hemisphere (healthy hemisphere) based on Anatomical Automatic Labeling atlas 3v1 (AAL3v1), to analyze the alteration in the healthy hemisphere. Other settings were consistent with the manual. Family-wise error (FWE) correction of peak level was performed for multiple comparison correction. A p-value < 0.05 was considered statistically significant.

Paired t-tests were performed with Gaussian random-field theory correction (voxel $p < 0.001$, cluster $p < 0.05$) for Reho, ALFF, and fALFF. The healthy hemisphere binary mask with voxel size matched was used to limit statistics to the healthy hemisphere. Paired t-tests of cognitive assessment scores were performed by SPSS (IBM SPSS Statistics version 24, IBM Corporation).

BrainNet Viewer toolbox (Xia et al., 2013) was used to present functional analysis results and xjView toolbox (https://www.alivelearn.net/xjview) to show VBM analysis results. No SBM analysis results

passed the multiple comparison correction. We chose AAL3v1 atlas to label names of significant regions (Rolls et al., 2020).

Results

Clinical Characteristics

Thirty-two patients were included (15 females, 46.88%) aged 5–18 (mean 9.84 ± 2.00 years) (Table 1). Initial symptom included seizures (n = 19), headache with or without concomitant symptoms (n = 7), facioplegia (n = 1), and vomiting (n = 1). Four patients showed no symptoms and the ISOLs were stumbled upon. Eleven cases involved the frontal lobe; nine, the temporal lobe; five, the parietal lobe; five, the posterior cranial fossa; and two, the occipital lobe. The lesion was present in the left hemisphere in 18 patients. Lesion volume could be approximately calculated using the formula for spheroid: $V = 4/3\pi \times a/2 \times b/2 \times c/2$ (a and b = maximum perpendicular diameters on the axial images; c = diameter in the coronal direction on the sagittal or coronal images) (Li et al., 2016; Osawa et al., 2013). The mean size of intracranial space-occupying mass was 11906.92 ± 18605.93 mm^3. Gross total resection rate was approximately 87.50%. The follow-up interval ranged from 4-143 days (mean 38.91 ± 42.71 days). The histopathological diagnosis results were presented in Supplementary Table 1. Among them, tumor accounted for 68.74%, vascular malformation for 21.88%, and the remaining comprised of non-tumor and non-vascular malformations for 9.4% (including one case of immune inflammation and two cases of brain tissue degeneration).

Table 1
Clinical characteristics of pediatric patients

	Value/Number	Percentage(%)
Age(mean ± SD)(years)*	9.84 ± 2.00	
Gender(male:female)	17:15	53.13:46.88
Initial Symptom		
Seizure	19	59.38
Only Headache	4	12.50
Asymptomatic	4	12.50
Headache with vomiting	2	6.25
Headache with dystaxia	1	3.13
Facioplegia	1	3.13
Only vomiting	1	3.13
Disease (Tumor:Vascular malformation:Not Tumor)	22:7:3	68.74:21.88:9.38
Lesion Lateralization (Left:Right)	18:14	56.25:43.75
Location of lesions		
Frontal (Left:right)	11 (6:5)	34.38
Parietal (Left:right)	5 (3:2)	15.63
Temporal (Left:right)	9 (6:3)	28.13
Occipital (Left:right)	2 (1:1)	6.25
Posterior fossa (Left:Right)	5 (2:3)	15.63
Lesion size(mean ± SD) mm^3 !	11906.92 ± 18605.93	
Degree of excision (Gross total:Subtotal)	28:4	87.50:12.50
Follow-up interval(mean ± SD) days $	38.91 ± 42.71	
* ranging from 5–18 years		
! the minimum of 148.7 mm3 and the maximum of 79521.0 mm3		
$ from the first postoperative day to the follow-up day, ranging from 4 days to 143 days.		

Brain Imaging Analysis

Patient with lesions on the right hemisphere had their scans flipped for convenience. Therefore, the healthy hemisphere of all patients is now the “right hemisphere” no matter which hemisphere it was originally. However, since the anatomical structure of the hemispheres is not completely symmetrical, we reported the corresponding locations of statistically significant regions and the number of voxels according to the respective hemisphere.

For postoperative versus preoperative data, there were four clusters of VBM analysis that passed the peak level FWE correction (Fig. 1, Table 2). The peak intensity of the four clusters was positive, which means that the GM volume in fusiform, triangular part of inferior frontal gyrus, superior frontal gyrus, and medial superior frontal gyrus of the healthy hemisphere increased postoperatively compared to before surgery. There was no statistical significance in preoperative versus postoperative comparisons. Similarly, for the four indices generated by SBM analysis, neither of the two contrast designs approached statistical significance, and no difference in thickness, depth, gyrification, and FD before and after operation was observed.

Table 2

Results of VBM analysis, Reho and fALFF*

	No. of clusters	No. of all voxels	Peak MNI coordinate(x,y,z)	Peak MNI coordinate region (Number. of voxels	Peak intensity
VBM	Cluster 1	8	(26,-44,-12)	Fusiform_R (7)/L# (8)	6.02
	Cluster 2	18	(38,29,-2)	Frontal_Inf_Tri_R (12)/L (15)	5.81
	Cluster 3	94	(29,60,8)	Frontal_Sup_2_R (92)/L (67)	6.75
	Cluster 4	34	(6,57,8)	Frontal_Sup_Medial_R (33)/L (34)	5.83
fALFF	Cluster 1	19	(33,-81,-51)	Cerebellum_Crus2_R (19)/None (12)	5.77
	Cluster 2	15	(30,21,54)	Frontal_Mid_2_R (6)/L (15)	5.38
	Cluster 3	12	(39,21,45)	Frontal_Mid_2_R (12)/L (12)	5.06
Reho	Cluster 1	16	(21,48,36)	Frontal_Sup_2_R (14)/L (15)	5.09

Fusiform_R: Fusiform gyrus, right; Frontal_Sup_2_R: Superior frontal gyrus, dorsolateral, right; Frontal_Sup_Medial_R: Superior frontal gyrus, medial, right; Frontal_Inf_Tri_L: Inferior frontal gyrus, triangular part, left; Cerebellum_Crus2_R: Crus II of cerebellar hemisphere, right; Frontal_Mid_2_R: Middle frontal gyrus, right

*The results shown in the table suggested that the corresponding indexes after surgery were higher than those before surgery.

#If activated regions have corresponding names in different hemispheres, we simply recorded the region on the left as "L" and attach the corresponding voxel number in the table. If activated regions in the left and right hemispheres don't match, then we write down the location name and the number of voxels in the left hemisphere.

We compared postoperative to preoperative Reho, ALFF, and fALFF, and found that only Reho and fALFF passed the correction (Fig. 2, Table 2). The peak intensity of all the masses was positive but not negative, indicating that the Reho and fALFF were increased in the corresponding brain regions after surgery compared with before surgery, and there was no decrease in any brain regions. These brain regions are mainly located in the frontal lobe, and their specific names are detailed in Table 2.

Three domains of the CNS VS were statistically significant i.e., psychomotor speed, motor speed, and reasoning. PsyMoSp and MS decreased after surgery, while reasoning increased. The calculation formula of PsyMoSp and MS was very similar, and the difference was only in symbol digit coding correct responses (SDC CR). PsyMoSp added an SDC CR score to this formula. We conducted a paired t-test for this score to further clarify this (Table 3).

Table 3
Cognitive assessment scores comparison (post-operative versus pre-operative, two-tailed)

Clinical Domain	mean	SD	T value	P value
NCI	-3.39	16.72	-0.97	0.34
Composite Memory	-4.78	26.34	-0.87	0.39
Verbal Memory	-0.44	29.63	-0.07	0.95
Visual Memory	-7.00	21.59	-1.56	0.13
Psychomotor Speed	-5.30	9.66	-2.63	**0.02**
Reaction Time	-5.87	20.07	-1.40	0.18
Complex Attention	-1.83	25.28	-0.35	0.73
Cognitive Flexibility	0.52	26.58	0.09	0.93
Processing Speed	-3.130	13.19	-1.14	0.27
Executive Function	0.91	25.78	0.17	0.87
Simple Attention	-5.00	31.43	-0.76	0.45
Motor Speed	-5.74	11.45	-2.40	**0.03**
Social Acuity	11.52	30.63	1.80	0.09
Reasoning	7.13	11.01	3.11	**0.01**
Sustained Attention	4.78	16.81	1.36	0.19
Working Memory	1.39	13.18	0.51	0.62
Symbol Digit Coding Correct Responses	-3.22	12.36	-1.25	0.23

Discussion

GM volume increases in some areas of the healthy hemisphere, mainly in the frontal lobe, in pediatric patients with heterogeneous tumors after surgery. The healthy hemisphere had some structural changes after operation; however, four indices of the SBM analysis did not pass correction, which might indicate that the GM volume measured by VBM is a composite result combining thickness, sulcus depth, gyrification, FD, and other indicators not provided by CAT12. This is the first study to demonstrate brain structural and functional changes in the healthy hemisphere after brain surgery in children within 6 months.

The mixed measurements increased sensitivity compared to analyses using each measurement method alone, which corroborated to a previous study (Voets et al., 2008). The main active brain region after surgery was the frontal lobe, which supported the fact that the frontal lobe was the main area of change. These functional and structural changes may be due to neuroplasticity mechanisms and can be explored and studied by means of brain imaging (Xu et al., 2017). Plasticity is the intrinsic adaptation of the central nervous system to changes in the internal and external environment. It occurs throughout the life cycle, during development, new learning, and adaptive mechanisms to support functional recovery after brain injury (Draganski et al., 2004; Maguire et al., 2000; Payne & Lomber, 2001). Therefore, after an injury, the brain activates its plasticity mechanisms to compensate to minimize the effects of the injury.

Our VBM and functional imaging analyses indicated that the compensation of the healthy hemisphere was mainly in the frontal lobe, especially the dorsolateral superior frontal gyrus. Liu et al. (Liu et al., 2020) found that unilateral frontal glioma invasion of the frontal lobe in adults caused structural and functional reorganization of the contralateral structure of the posterior cognitive control network, especially the contralateral superior parietal lobe. While results in insular glioma adult patients supports the plasticity mechanism of homologous recombination which means the damage of the lesion side brain region was compensated by the corresponding brain region of the healthy side (Almairac et al., 2018), ours results differ, as do the compensatory brain regions. There may be differences in the mechanisms of plasticity between adults and children that have influenced the results. With regards to GM density/volume during brain development (Sowell et al., 2001), the local decrease in GM density is mainly distributed in the dorsal frontal and parietal lobes during childhood and adolescence. Additionally, between adolescence and adulthood, a sharp increase in local GM density in the frontal lobe is observed (Sowell et al., 2001). Further, the loss of GM in the parietal lobe decreases relative to the early period. We found that GM density decreases in the dorsal frontal and parietal lobes as a developmental trend toward maturity from childhood to adolescence. In adult development, frontal lobe density increases and parietal lobe density decreases, which implies that there are structural changes in different brain regions at different ages. Conversely, increased GM density in the dorsal frontal or parietal lobes in children and adolescents after a certain treatment may represent reduced maturity in that region, or reverse development. We found increased GM density/volume in the frontal lobe. Therefore, the mechanism of the plasticity recombination of the healthy hemisphere after focal injury in children may be to reduce the

developmental stage of some brain regions of the frontal lobe, to promote functional compensation and functional recombination, and reduce the impact of surgical injury.

For brain damage in adults, an increase in GM density/volume might be observed in the parietal lobe (Liu et al., 2020). GM volume in the healthy parietal lobe increased significantly when the tumor invaded the right frontal lobe compared with the control group. Although this phenomenon is is only found in one hemisphere, it is in line with our findings. This developmental stage difference may be one of the reasons for the difference in postoperative compensation between adults and children. Some studies support our hypothesis, and events that occur after injury are similar to those observed during normal development (Cramer & Chopp, 2000; Dromerick et al., 2015; Kollen et al., 2009; Pollock et al., 2007; Shehadah et al., 2014; Zeiler et al., 2016). However, Xu et al. (Xu et al., 2017) found compensatory sites in the right cuneus, left thalamus, and right globus pallidus in glioma adult patients, and Huang et al. (Huang et al., 2021) found increased contralateral insula GM volume in glioma adult patients with IDH mutations. These results cannot be well explained by our theory since the influencing factors are complex; hence, further research is needed in this regard.

Previous studies on brain structure changes in survivors of pediatric brain tumor focused on posterior fossa tumors, and few investigated only surgical injuries (Ailion et al., 2017); however, most of them investigated the combined effects of surgery, chemotherapy, and radiotherapy. Horská et al. (Horská et al., 2010) investigated the volume changes of the vermis of the cerebellum in tumor patients, and found that the volume decreased after surgery, radiation, or chemotherapy. Leung et al. (Leung et al., 2004) conducted a study on a similar cohort, and found that the integrity of several white matter areas in the whole brain decreased after treatment. Jayakar et al. (Jayakar et al., 2015) observed a decrease in bilateral hippocampal, putamen, and whole brain volume in pediatric patients after undergoing radiation or chemotherapy. Patients in these studies experienced extensive brain damage, such as that following radiotherapy or chemotherapy. Further, the GM and WM were damaged, which differs from the results of structural compensation in our study. We hypothesize that focal injury can stimulate structural compensation in the brain. However, if the damage pattern is too extensive, it is difficult to compensate within the structure.

Extensive atrophy of the WM was also found in a study of TBI (Dennis et al., 2017). Interhemispheric transfer time, measured as an event-related potential, was used to divide patients into a TBI-slow group and a TBI-normal group. Some areas of the TBI-slow group, such as the superior frontal gyrus, had increased GM volume compared with the TBI-normal group. The WM damage in the TBI-slow group was more severe than that in the TBI-normal group, and the more severely damaged group showed an increase in GM volume. All our surgical patients suffered WM damage, and GM volume increased in the healthy hemisphere, which was similar to the aforementioned results. We assume that focal WM injury may increase GM volume in some areas of the brain to reduce the effects of injury. However, if the damage scope is too wide, this mechanism may not exist.

For the cognitive assessment, PsyMoSp measures how well a subject perceives, attends, responds to visual-perceptual information, and performs motor speed and fine motor coordination; and MS measures the ability to perform movements to produce and satisfy an intention toward a manual action and goal. Further, MS can influence PsyMoSp. The difference in calculation of these two indicators lies in the score of SDC CR, which we compared with no statistical difference using paired T-test (Table 3). The decline in motor speed may cause a decline in psychomotor speed, and other cognitive functions required by psychomotor speed have not been impaired or have been restored. However, there were no corresponding brain imaging results in the healthy hemisphere to explain this phenomenon, which may be caused by surgical injury in the affected hemisphere.

There is a period of vulnerability after brain damage (Madhavan et al., 2019). From the perspective of the whole brain, the decline of PsyMoSp could indicate that the brain is in a vulnerable stage (Amieva et al., 2019). As for the reasoning score, the battery uses a non-verbal reasoning test to assess reasoning ability, which is a higher cognitive function mainly involving the frontal lobe (Dosenbach et al., 2010; Paz-Alonso et al., 2014; Soderqvist et al., 2012). Our results showed structural and functional changes in the healthy frontal lobe, which is consistent with the trend of reasoning score changes after surgery. There is sufficient evidence that substantial spontaneous recovery occurs weeks or months after the sudden onset of brain injury, including cognitive ability (Fasotti, 2017). Therefore, we hypothesize that the recovery of some higher cognitive functions can be seen within 6 months after brain surgery in children, and the related brain regions are mainly in the frontal lobe.

The current study had some limitations. The unwillingness of the guardians of the children to cooperate with follow-up made it challenging to acquire more extended follow-up data. Additionally, the participants' poor self-control made it harder to minimize head movements in the lengthy MRI scan, resulting in incomplete data. Further studies could redo the rs-fMRI scan, retest to understand the changes after 6 months, and expand the sample size to reduce the effects of noise.

Conclusion

In children and adolescents, GM volume increased in some areas of the healthy hemisphere, mainly in the frontal lobe, within 6 months after surgery for ISOLs. The frontal lobe was the main functionally active region. Structural and functional compensation may occur in the healthy hemisphere within 6 months after surgery for ISOLs in children and adolescents, and the healthy hemisphere is primarily responsible for compensating for the effects of surgical injury, especially for some higher cognitive function. At the macro level, this compensation may primarily occur in the frontal lobe. Our results further suggest that brain surgery in children has little impact on higher cognitive function and may lead to some degree of self-compensation. Our conclusion may provide some guidance for the rehabilitation of children after brain surgery.

Declarations

Acknowledgements

My effusive thanks to Shihao He for help and support during my studies. I couldn't have done the research without his guidance. Thanks to my mentor and his team for their trust and support.

Funding

This research was funded by the National Natural Science Foundation of China (No.81870834) and the Special project of peadiatrics of collaborative development centre of Beijing hospital administration (No. XTYB201817).

Conflicts of interest

The authors declare that the research was conducted in the absence of any commercial or financial relationships that could be construed as a potential conflict of interest.

Ethics approval

Written informed consent was obtained from all enrolled pediatric patients' parents. This prospective study was performed in line with the principles of the Declaration of Helsinki and was approved by the Institutional Review Board of Beijing Tiantan Hospital, Capital Medical University (KY 2021-100-02).

Consent to participate

All participants had given their informed written consent.

Consent to publish

Not applicable

Availability of data and materials

All data generated or analyzed during this study are included in the published article. Some or all data, models, or code generated or used during the study are available from the corresponding author by request.

Code availability

Applicable.

Author Contributions

Author contributions included conception and study design (XY Guan, WJ Zheng and J Gong), data collection or acquisition (XY Guan, KY Fan, X Han, Z Lu and BH Hu), statistical analysis (XY Guan, WJ Zheng, X Han, ZH Yan, and X Li), interpretation of results (XY Guan and WJ Zheng), drafting the manuscript work or revising it critically for important intellectual content (XY Guan, WJ Zheng, Z Lu and J

Gong) and approval of final version to be published and agreement to be accountable for the integrity and accuracy of all aspects of the work (All authors).

References

1. Ailion, A. S., Hortman, K., & King, T. Z. (2017). Childhood Brain Tumors: a Systematic Review of the Structural Neuroimaging Literature. *Neuropsychology Review*, *27*(3), 220–244. https://doi.org/10.1007/s11065-017-9352-6
2. Almairac, F., Duffau, H., & Herbet, G. (2018). Contralesional macrostructural plasticity of the insular cortex in patients with glioma: A VBM study. *Neurology*, *91*(20), e1902-e1908. https://doi.org/10.1212/WNL.0000000000006517
3. Amieva, H., Meillon, C., Proust-Lima, C., & Dartigues, J. F. (2019). Is Low Psychomotor Speed a Marker of Brain Vulnerability in Late Life? Digit Symbol Substitution Test in the Prediction of Alzheimer, Parkinson, Stroke, Disability, and Depression. *Dementia And Geriatric Cognitive Disorders*, *47*(4–6), 297–305. https://doi.org/10.1159/000500597
4. Ashburner, J. (2007). A fast diffeomorphic image registration algorithm. *Neuroimage*, *38*(1), 95–113. https://doi.org/10.1016/j.neuroimage.2007.07.007
5. Ashburner, J., & Friston, K. J. (2005). Unified segmentation. *Neuroimage*, *26*(3), 839–851. https://doi.org/10.1016/j.neuroimage.2005.02.018
6. Chao-Gan, Y., & Yu-Feng, Z. (2010). DPARSF: A MATLAB Toolbox for "Pipeline" Data Analysis of Resting-State fMRI. *Frontiers In Systems Neuroscience*, *4*, 13. https://doi.org/10.3389/fnsys.2010.00013
7. Cramer, S. C., & Chopp, M. (2000). Recovery recapitulates ontogeny. *Trends In Neurosciences*, *23*(6), 265–271
8. Dennis, E. L., Faskowitz, J., Rashid, F., Babikian, T., Mink, R., Babbitt, C., & Asarnow, R. F. (2017). Diverging volumetric trajectories following pediatric traumatic brain injury. *Neuroimage Clin*, *15*, 125–135. https://doi.org/10.1016/j.nicl.2017.03.014
9. Dosenbach, N. U., Nardos, B., Cohen, A. L., Fair, D. A., Power, J. D., Church, J. A., & Schlaggar, B. L. (2010). Prediction of individual brain maturity using fMRI. *Science*, *329*(5997), 1358–1361. https://doi.org/10.1126/science.1194144
10. Draganski, B., Gaser, C., Busch, V., Schuierer, G., Bogdahn, U., & May, A. (2004). Changes in grey matter induced by training. *Nature*, *427*(6972), 311–312. https://doi.org/10.1038/427311a
11. Dromerick, A. W., Edwardson, M. A., Edwards, D. F., Giannetti, M. L., Barth, J., Brady, K. P., & Newport, E. L. (2015). Critical periods after stroke study: translating animal stroke recovery experiments into a clinical trial. *Frontiers In Human Neuroscience*, *9*, 231. https://doi.org/10.3389/fnhum.2015.00231
12. Fasotti, L. (2017). Mechanisms of recovery after acquired brain injury. *Neuropsychol Rehabil* (pp. 25–35). Routledge

13. Friston, K. J., Williams, S., Howard, R., Frackowiak, R. S., & Turner, R. (1996). Movement-related effects in fMRI time-series. *Magnetic Resonance In Medicine*, *35*(3), 346–355. https://doi.org/10.1002/mrm.1910350312
14. Gualtieri, C., & Johnson, L. (2006). Reliability and validity of a computerized neurocognitive test battery, CNS Vital Signs. *Archives of Clinical Neuropsychology*, *21*(7), 623–643. https://doi.org/10.1016/j.acn.2006.05.007
15. He, H., & Liu, T. T. (2012). A geometric view of global signal confounds in resting-state functional MRI. *Neuroimage*, *59*(3), 2339–2348. https://doi.org/10.1016/j.neuroimage.2011.09.018
16. Horská, A., Laclair, A., Mohamed, M., Wells, C. T., McNutt, T., Cohen, K. J., & Kates, W. (2010). Low cerebellar vermis volumes and impaired neuropsychologic performance in children treated for brain tumors and leukemia. *Ajnr. American Journal Of Neuroradiology*, *31*(8), 1430–1437. https://doi.org/10.3174/ajnr.A2114
17. Huang, Z., Li, G., Li, Z., Sun, S., Zhang, Y., Hou, Z., & Xie, J. (2021). Contralesional Structural Plasticity in Different Molecular Pathologic Subtypes of Insular Glioma. *Frontiers In Neurology*, *12*, 636573. https://doi.org/10.3389/fneur.2021.636573
18. Jayakar, R., King, T. Z., Morris, R., & Na, S. (2015). Hippocampal volume and auditory attention on a verbal memory task with adult survivors of pediatric brain tumor. *Neuropsychology*, *29*(2), 303–319. https://doi.org/10.1037/neu0000183
19. Kollen, B. J., Lennon, S., Lyons, B., Wheatley-Smith, L., Scheper, M., Buurke, J. H., & Kwakkel, G. (2009). The effectiveness of the Bobath concept in stroke rehabilitation: what is the evidence? *Stroke*, *40*(4), e89–97. https://doi.org/10.1161/strokeaha.108.533828
20. Lee, M. H., Smyser, C. D., & Shimony, J. S. (2013). Resting-State fMRI: A Review of Methods and Clinical Applications [Review]. *American Journal of Neuroradiology*, *34*(10), 1866–1872. https://doi.org/10.3174/ajnr.A3263
21. Leung, L. H., Ooi, G. C., Kwong, D. L., Chan, G. C., Cao, G., & Khong, P. L. (2004). White-matter diffusion anisotropy after chemo-irradiation: a statistical parametric mapping study and histogram analysis. *Neuroimage*, *21*(1), 261–268. https://doi.org/10.1016/j.neuroimage.2003.09.020
22. Li, H., Zhao, M., Wang, S., Cao, Y., & Zhao, J. (2016). Prediction of pediatric meningioma recurrence by preoperative MRI assessment. *Neurosurgical Review*, *39*(4), 663–669. https://doi.org/10.1007/s10143-016-0716-9
23. Liu, Y., Hu, G., Yu, Y., Jiang, Z., Yang, K., Hu, X., & Chen, J. (2020). Structural and Functional Reorganization Within Cognitive Control Network Associated With Protection of Executive Function in Patients With Unilateral Frontal Gliomas. *Frontiers In Oncology*, *10*, 794. https://doi.org/10.3389/fonc.2020.00794
24. Louis, D. N., Perry, A., Reifenberger, G., von Deimling, A., Figarella-Branger, D., Cavenee, W. K., & Ellison, D. W. (2016). The 2016 World Health Organization Classification of Tumors of the Central Nervous System: a summary. *Acta Neuropathologica*, *131*(6), 803–820. https://doi.org/10.1007/s00401-016-1545-1

25. Louis, D. N., Perry, A., Wesseling, P., Brat, D. J., Cree, I. A., Figarella-Branger, D., & Ellison, D. W. (2021). The 2021 WHO Classification of Tumors of the Central Nervous System: a summary. *Neuro Oncol*, *23*(8), 1231–1251. https://doi.org/10.1093/neuonc/noab106
26. Lv, H., Wang, Z., Tong, E., Williams, L. M., Zaharchuk, G., Zeineh, M., & Wintermark, M. (2018). Resting-State Functional MRI: Everything That Nonexperts Have Always Wanted to Know. *Ajnr. American Journal Of Neuroradiology*, *39*(8), 1390–1399. https://doi.org/10.3174/ajnr.A5527
27. Madhavan, R., Joel, S. E., Mullick, R., Cogsil, T., Niogi, S. N., Tsiouris, A. J., & Shetty, T. (2019). Longitudinal Resting State Functional Connectivity Predicts Clinical Outcome in Mild Traumatic Brain Injury [Article]. *Journal Of Neurotrauma*, *36*(5), 650–660. https://doi.org/10.1089/neu.2018.5739
28. Maguire, E. A., Gadian, D. G., Johnsrude, I. S., Good, C. D., Ashburner, J., Frackowiak, R. S., & Frith, C. D. (2000). Navigation-related structural change in the hippocampi of taxi drivers. *Proc Natl Acad Sci U S A*, *97*(8), 4398–4403. https://doi.org/10.1073/pnas.070039597
29. Osawa, T., Tosaka, M., Nagaishi, M., & Yoshimoto, Y. (2013). Factors affecting peritumoral brain edema in meningioma: special histological subtypes with prominently extensive edema. *Journal Of Neuro-Oncology*, *111*(1), 49–57. https://doi.org/10.1007/s11060-012-0989-y
30. Ostrom, Q. T., Cioffi, G., Waite, K., Kruchko, C., & Barnholtz-Sloan, J. S. (2021). CBTRUS Statistical Report: Primary Brain and Other Central Nervous System Tumors Diagnosed in the United States in 2014–2018. *Neuro Oncol*, *23*(12 Suppl 2), iii1–iii105. https://doi.org/10.1093/neuonc/noab200
31. Payne, B. R., & Lomber, S. G. (2001). Reconstructing functional systems after lesions of cerebral cortex. *Nature Reviews Neuroscience*, *2*(12), 911–919. https://doi.org/10.1038/35104085
32. Paz-Alonso, P. M., Bunge, S. A., & Ghetti, S. (2014). *Emergence of higher cognitive functions: Reorganization of largescale brain networks during childhood and adolescence*. In: Oxford Handbooks Online
33. Pollock, A., Baer, G., Pomeroy, V., & Langhorne, P. (2007). Physiotherapy treatment approaches for the recovery of postural control and lower limb function following stroke. *Cochrane Database Systematic Review*, (1), Cd001920. https://doi.org/10.1002/14651858.CD001920.pub2
34. Rolls, E. T., Huang, C. C., Lin, C. P., Feng, J., & Joliot, M. (2020). Automated anatomical labelling atlas 3. *Neuroimage*, *206*, 116189. https://doi.org/10.1016/j.neuroimage.2019.116189
35. Saad, Z. S., Gotts, S. J., Murphy, K., Chen, G., Jo, H. J., Martin, A., & Cox, R. W. (2012). Trouble at Rest: How Correlation Patterns and Group Differences Become Distorted After Global Signal Regression. *Brain Connectivity*, *2*(1), 25–32. https://doi.org/10.1089/brain.2012.0080
36. Shehadah, A., Chen, J., Pal, A., He, S., Zeitlin, A., Cui, X., & Chopp, M. (2014). Human placenta-derived adherent cell treatment of experimental stroke promotes functional recovery after stroke in young adult and older rats. *PLoS One*, *9*(1), e86621. https://doi.org/10.1371/journal.pone.0086621
37. Smitha, K. A., Raja, A., Arun, K., Rajesh, K. M., Thomas, P. G., Kapilamoorthy, B., T. R., & Kesavadas, C. (2017). Resting state fMRI: A review on methods in resting state connectivity analysis and resting

state networks. *The Neuroradiology Journal*, *30*(4), 305–317. https://doi.org/10.1177/1971400917697342

38. Soderqvist, S., Nutley, S. B., Ottersen, J., Grill, K. M., & Klingberg, T. (2012). Computerized training of non-verbal reasoning and working memory in children with intellectual disability. *Frontiers In Human Neuroscience*, *6*, 271. https://doi.org/10.3389/fnhum.2012.00271
39. Sowell, E. R., Thompson, P. M., Tessner, K. D., & Toga, A. W. (2001). Mapping Continued Brain Growth and Gray Matter Density Reduction in Dorsal Frontal Cortex: Inverse Relationships during Postadolescent Brain Maturation. *The Journal of Neuroscience*, *21*(22), 8819–8829. https://doi.org/10.1523/jneurosci.21-22-08819.2001
40. Voets, N. L., Hough, M. G., Douaud, G., Matthews, P. M., James, A., Winmill, L., & Smith, S. (2008). Evidence for abnormalities of cortical development in adolescent-onset schizophrenia. *Neuroimage*, *43*(4), 665–675. https://doi.org/10.1016/j.neuroimage.2008.08.013
41. Whitwell, J. L. (2009). Voxel-based morphometry: an automated technique for assessing structural changes in the brain. *Journal Of Neuroscience*, *29*(31), 9661–9664. https://doi.org/10.1523/JNEUROSCI.2160-09.2009
42. Xia, M., Wang, J., & He, Y. (2013). BrainNet Viewer: a network visualization tool for human brain connectomics. *PLoS One*, *8*(7), e68910. https://doi.org/10.1371/journal.pone.0068910
43. Xu, J., Elazab, A., Liang, J., Jia, F., Zheng, H., Wang, W., & Hu, Q. (2017). Cortical and Subcortical Structural Plasticity Associated with the Glioma Volumes in Patients with Cerebral Gliomas Revealed by Surface-Based Morphometry. *Frontiers In Neurology*, *8*, 266. https://doi.org/10.3389/fneur.2017.00266
44. Yan, C. G., Wang, X. D., Zuo, X. N., & Zang, Y. F. (2016). DPABI: Data Processing & Analysis for (Resting-State)Brain Imaging. Neuroinformatics, 14(3),339–351. https://doi.org/10.1007/s12021-016-9299-4
45. Ying, J., Yuan, T., Jin, L., Li, C., Gui, S., Wang, R., & Zhang, Y. (2020). Brain Morphometric and Functional Magnetic Resonance Imaging Study on Patients with Visual Field Defects Resulting from Suprasellar Tumors: Preoperative and Postoperative Assessment. *World Neurosurg*, *134*, e353–e359. https://doi.org/10.1016/j.wneu.2019.10.060
46. Zeiler, S. R., Hubbard, R., Gibson, E. M., Zheng, T., Ng, K., O'Brien, R., & Krakauer, J. W. (2016). Paradoxical Motor Recovery From a First Stroke After Induction of a Second Stroke: Reopening a Postischemic Sensitive Period. *Neurorehabil Neural Repair*, *30*(8), 794–800. https://doi.org/10.1177/1545968315624783
47. Zhao, T., Liao, X., Fonov, V. S., Wang, Q., Men, W., Wang, Y., & He, Y. (2019). Unbiased age-specific structural brain atlases for Chinese pediatric population. *Neuroimage*, *189*, 55–70. https://doi.org/10.1016/j.neuroimage.2019.01.006

Figures

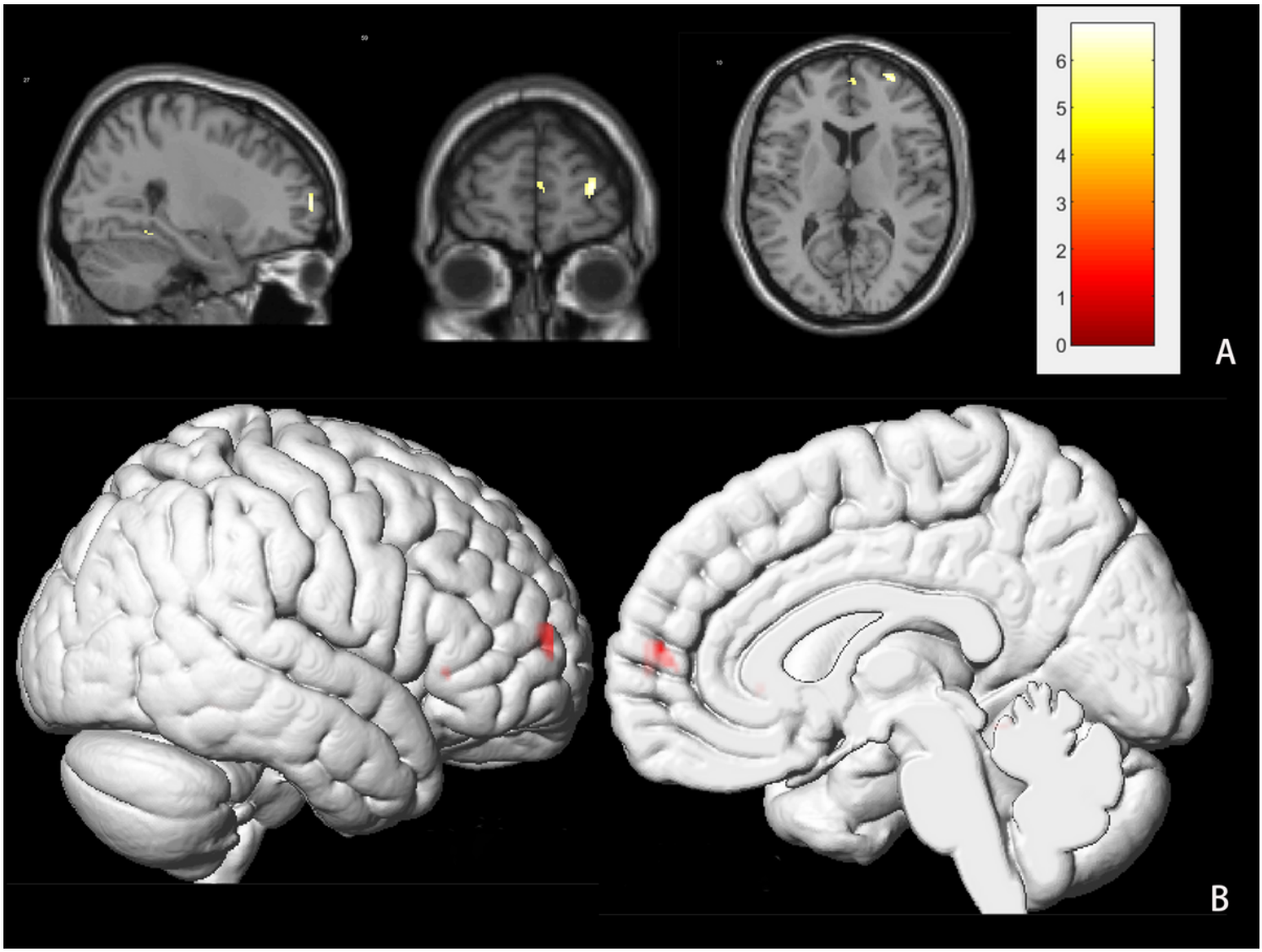

Figure 1

VBM analysis results (post-operative versus pre-operative).

VBM analysis showed that the GM volume in fusiform gyrus, triangular part of inferior frontal gyrus, dorsolateral superior frontal gyrus, and medial superior frontal gyrus increased significantly after operation. The increase in GM volume was mainly located in the frontal lobe. Figure 1 A shows active brain regions from sagittal, coronal, and axial positions, with colorbar attached. Figure 1 B is a macroscopic representation of the activated brain regions in three dimensions.

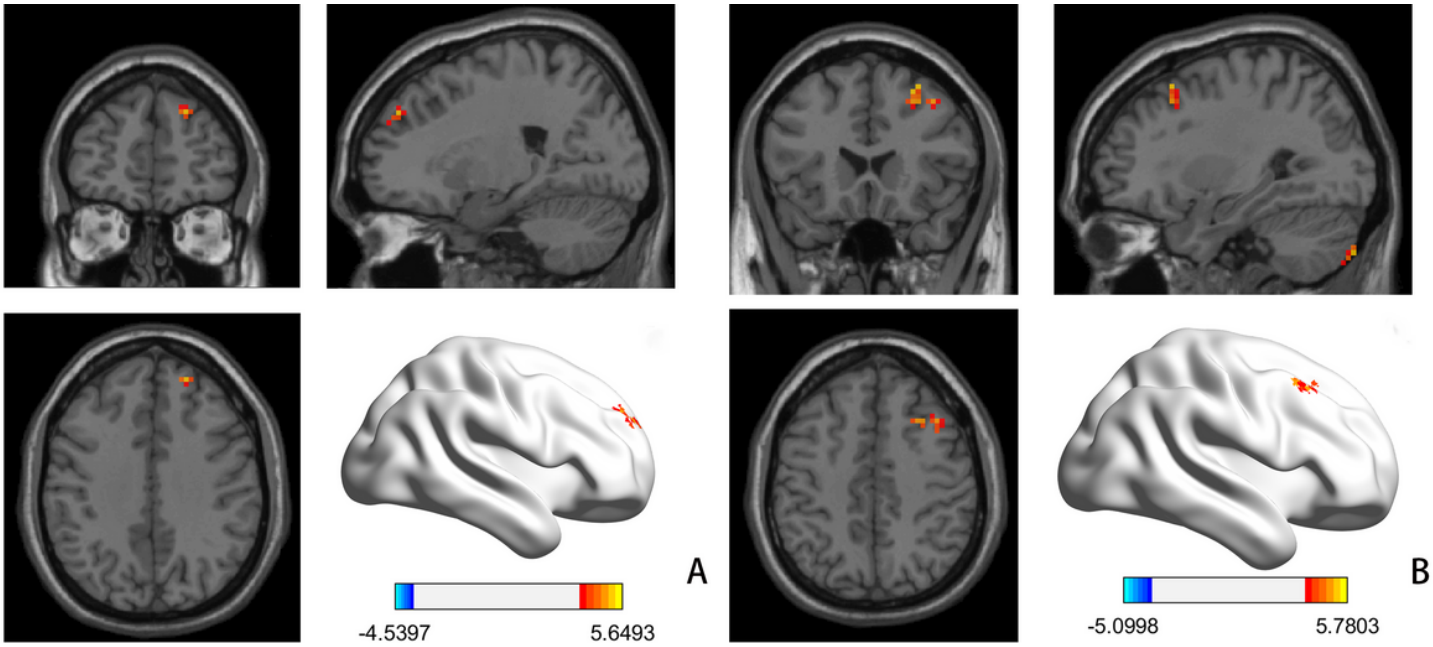

Figure 2

Reho and fALFF results (post-operative versus pre-operative)

A: Reho results: The results of Reho suggested that the activation of the medial superior frontal gyrus was significantly higher after surgery than before

B: fALFF results: The results of fALFF showed that the activation of the middle frontal gyrus and Crus II of cerebellar hemisphere was significantly higher after surgery than before

Supplementary Files

This is a list of supplementary files associated with this preprint. Click to download.

- AuthorChecklist11682.pdf
- Supplementarymaterials.docx